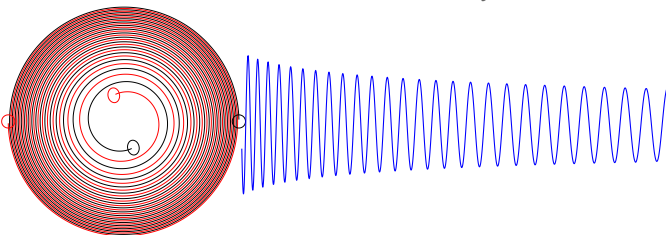


Numerical Simulations of Black Hole Spacetimes

Lee Lindblom

Senior Research Associate
Theoretical Astrophysics

Physics Research Conference
California Institute of Technology
24 May 2007



● Caltech-Cornell Numerical Relativity Collaboration

Group leaders: Lee Lindblom, Mark Scheel, and Harald Pfeiffer at Caltech; Saul Teukolsky and Larry Kidder at Cornell.



Kidder



Lindblom



Pfeiffer



Scheel



Teukolsky

- **Caltech-Cornell Numerical Relativity Collaboration**

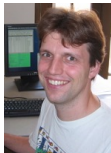
Group leaders: Lee Lindblom, Mark Scheel, and Harald Pfeiffer at Caltech; Saul Teukolsky and Larry Kidder at Cornell.



Kidder



Lindblom



Pfeiffer



Scheel



Teukolsky

- **Caltech** group: Michael Boyle, Jeandrew Brink, Duncan Brown, Tony Chu, Michael Cohen, Lee Lindblom, Geoffrey Lovelace, Keith Matthews, Robert Owen, Harald Pfeiffer, Oliver Rinne, Mark Scheel, Kip Thorne.
- **Cornell** group: Matthew Duez, Francois Foucart, Lawrence Kidder, Francois Limousin, Abdul Mroue, Nick Taylor, Saul Teukolsky, James York.

Motivation: Gravitational Wave Astronomy

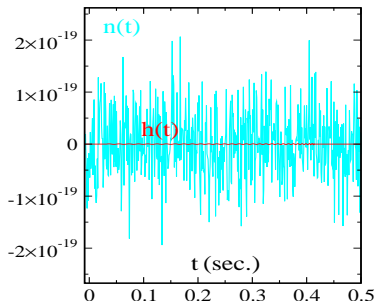
- Recent work in numerical relativity is aimed at providing model waveforms for gravitational wave (GW) astronomy (LIGO, etc.).

Motivation: Gravitational Wave Astronomy

- Recent work in numerical relativity is aimed at providing model waveforms for gravitational wave (GW) astronomy (LIGO, etc.).
- Binary black hole systems emit large amounts of GW as the holes inspiral and ultimately merge. These are expected to be among the strongest sources detectable by LIGO.

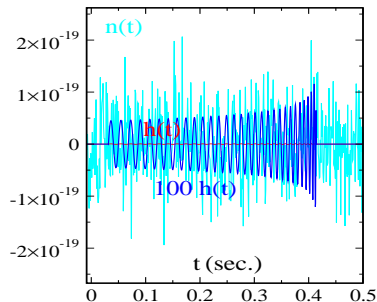
Motivation: Gravitational Wave Astronomy

- Recent work in numerical relativity is aimed at providing model waveforms for gravitational wave (GW) astronomy (LIGO, etc.).
- Binary black hole systems emit large amounts of GW as the holes inspiral and ultimately merge. These are expected to be among the strongest sources detectable by LIGO.
- Numerical waveforms may be useful in detection (to construct better data filters), and/or in modeling detected signals.



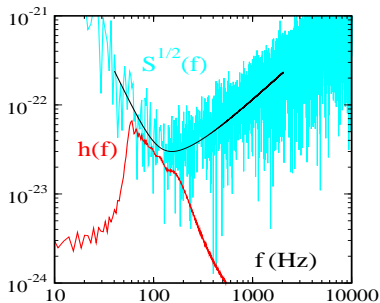
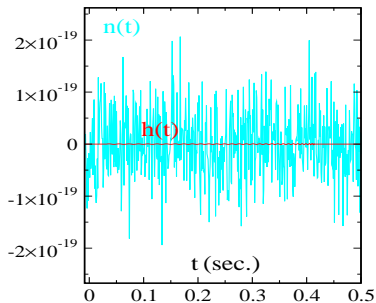
Motivation: Gravitational Wave Astronomy

- Recent work in numerical relativity is aimed at providing model waveforms for gravitational wave (GW) astronomy (LIGO, etc.).
- Binary black hole systems emit large amounts of GW as the holes inspiral and ultimately merge. These are expected to be among the strongest sources detectable by LIGO.
- Numerical waveforms may be useful in detection (to construct better data filters), and/or in modeling detected signals.



Motivation: Gravitational Wave Astronomy

- Recent work in numerical relativity is aimed at providing model waveforms for gravitational wave (GW) astronomy (LIGO, etc.).
- Binary black hole systems emit large amounts of GW as the holes inspiral and ultimately merge. These are expected to be among the strongest sources detectable by LIGO.
- Numerical waveforms may be useful in detection (to construct better data filters), and/or in modeling detected signals.



Why Is Numerical Relativity So Difficult?

- Dynamics of binary black hole problem is driven by delicate adjustments to orbit due to emission of gravitational waves.
- Very big computational problem:
 - Must evolve ~ 50 dynamical fields (spacetime metric plus all first derivatives).
 - Must accurately resolve features on many scales from black hole horizons $r \sim GM/c^2$ to emitted waves $r \sim 100GM/c^2$.
 - Many grid points are required $\gtrsim 10^6$ even if points are located optimally.

Why Is Numerical Relativity So Difficult?

- Dynamics of binary black hole problem is driven by delicate adjustments to orbit due to emission of gravitational waves.
- Very big computational problem:
 - Must evolve ~ 50 dynamical fields (spacetime metric plus all first derivatives).
 - Must accurately resolve features on many scales from black hole horizons $r \sim GM/c^2$ to emitted waves $r \sim 100GM/c^2$.
 - Many grid points are required $\gtrsim 10^6$ even if points are located optimally.
- Most representations of the Einstein equations have mathematically ill-posed initial value problems.
- Constraint violating instabilities destroy stable numerical solutions in many well-posed forms of the equations.

Unstable BBH Movie

Recent Progress in Numerical Relativity

- Frans Pretorius performs first numerical BBH inspiral, merger and ringdown calculations in the spring of 2005 using a “generalized harmonic” formulation of the Einstein equations. Pretorius Inspiral Movie

Recent Progress in Numerical Relativity

- Frans Pretorius performs first numerical BBH inspiral, merger and ringdown calculations in the spring of 2005 using a “generalized harmonic” formulation of the Einstein equations. Pretorius Inspiral Movie
- Groups at NASA GSFC and U. Texas–Brownsville simultaneously announce similar BBH simulations in the fall of 2005 using very different methods (BSSN–puncture).
LSU/AEI collaboration obtains similar results in Dec. 2005.
- Penn State group begins the study of physical properties of BBH orbits in early 2006 by evolving unequal mass binaries and measuring the kick velocity using BSSN–puncture methods.
- ...

Outline of Remainder of Talk:

- Three technical issues:
 - Constraint Damping.
 - Spectral Methods.
 - Feedback Control Systems.

- Interesting binary black hole simulations.

Gauge and Constraints in Electromagnetism

- The usual representation of the vacuum Maxwell equations split into evolution equations and constraints:

$$\begin{aligned}\partial_t \vec{E} &= \vec{\nabla} \times \vec{B}, & \nabla \cdot \vec{E} &= 0, \\ \partial_t \vec{B} &= -\vec{\nabla} \times \vec{E}, & \nabla \cdot \vec{B} &= 0.\end{aligned}$$

These equations are often written in the more compact 4-dimensional notation: $\nabla^a F_{ab} = 0$ and $\nabla_{[a} F_{bc]} = 0$, where F_{ab} has components \vec{E} and \vec{B} .

Gauge and Constraints in Electromagnetism

- The usual representation of the vacuum Maxwell equations split into evolution equations and constraints:

$$\begin{aligned}\partial_t \vec{E} &= \vec{\nabla} \times \vec{B}, & \nabla \cdot \vec{E} &= 0, \\ \partial_t \vec{B} &= -\vec{\nabla} \times \vec{E}, & \nabla \cdot \vec{B} &= 0.\end{aligned}$$

These equations are often written in the more compact 4-dimensional notation: $\nabla^a F_{ab} = 0$ and $\nabla_{[a} F_{bc]} = 0$, where F_{ab} has components \vec{E} and \vec{B} .

- Maxwell's equations are often re-expressed in terms of a vector potential $F_{ab} = \nabla_a A_b - \nabla_b A_a$:

$$\nabla^a \nabla_a A_b - \nabla_b \nabla^a A_a = 0.$$

Gauge and Constraints in Electromagnetism

- The usual representation of the vacuum Maxwell equations split into evolution equations and constraints:

$$\begin{aligned}\partial_t \vec{E} &= \vec{\nabla} \times \vec{B}, & \nabla \cdot \vec{E} &= 0, \\ \partial_t \vec{B} &= -\vec{\nabla} \times \vec{E}, & \nabla \cdot \vec{B} &= 0.\end{aligned}$$

These equations are often written in the more compact 4-dimensional notation: $\nabla^a F_{ab} = 0$ and $\nabla_{[a} F_{bc]} = 0$, where F_{ab} has components \vec{E} and \vec{B} .

- Maxwell's equations are often re-expressed in terms of a vector potential $F_{ab} = \nabla_a A_b - \nabla_b A_a$:

$$\nabla^a \nabla_a A_b - \nabla_b \nabla^a A_a = 0.$$

- This form of Maxwell's equations is manifestly hyperbolic as long as the gauge is chosen correctly, e.g., let $\nabla^a A_a = H(x, t)$, giving:

$$\nabla^a \nabla_a A_b \equiv \left(-\partial_t^2 + \partial_x^2 + \partial_y^2 + \partial_z^2 \right) A_b = \nabla_b H.$$

Constraint Damping

- Where are the constraints: $\nabla^a \nabla_a A_b = \nabla_b H$?

Constraint Damping

- Where are the constraints: $\nabla^a \nabla_a A_b = \nabla_b H$?
- Gauge condition becomes a constraint: $0 = \mathcal{C} \equiv \nabla^a A_a - H$.
- Maxwell's equations imply that this constraint is preserved:

$$\nabla^a \nabla_a \mathcal{C} = 0.$$

Constraint Damping

- Where are the constraints: $\nabla^a \nabla_a A_b = \nabla_b H$?
- Gauge condition becomes a constraint: $0 = \mathcal{C} \equiv \nabla^a A_a - H$.
- Maxwell's equations imply that this constraint is preserved:

$$\nabla^a \nabla_a \mathcal{C} = 0.$$

- Modify evolution equations by adding multiples of the constraints:

$$\nabla^a \nabla_a A_b = \nabla_b H + \gamma_0 t_b \mathcal{C} = \nabla_b H + \gamma_0 t_b (\nabla^a A_a - H).$$

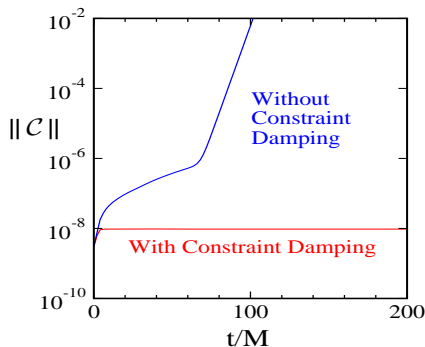
- These changes also affect the constraint evolution equation,

$$\nabla^a \nabla_a \mathcal{C} - \gamma_0 t^b \nabla_b \mathcal{C} = 0,$$

so constraint violations are damped when $\gamma_0 > 0$.

Constraint Damped Einstein System

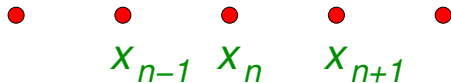
- “Generalized Harmonic” form of Einstein’s equations have properties similar to Maxwell’s equations:
 - Gauge (coordinate) conditions are imposed by specifying the divergence of the spacetime metric: $\partial_a g^{ab} = H^b + \dots$
 - Evolution equations become manifestly hyperbolic: $\square g_{ab} = \dots$
 - Gauge conditions become constraints.
 - Constraint damping terms can be added which make numerical evolutions stable.



Numerical Solution of Evolution Equations

$$\partial_t u = F(u, \partial_x u, x, t).$$

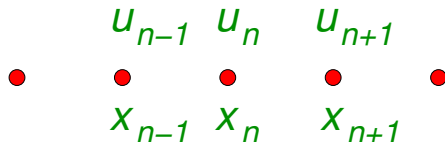
- Choose a grid of spatial points, x_n .



Numerical Solution of Evolution Equations

$$\partial_t u = F(u, \partial_x u, x, t).$$

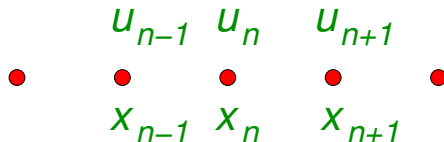
- Choose a grid of spatial points, x_n .
- Evaluate the function u on this grid: $u_n(t) = u(x_n, t)$.



Numerical Solution of Evolution Equations

$$\partial_t u = F(u, \partial_x u, x, t).$$

- Choose a grid of spatial points, x_n .
- Evaluate the function u on this grid: $u_n(t) = u(x_n, t)$.



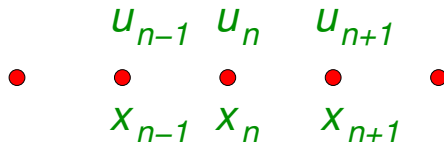
- Approximate the spatial derivatives at the grid points

$$\partial_x u(x_n) = \sum_k D_{nk} u_k.$$

Numerical Solution of Evolution Equations

$$\partial_t u = F(u, \partial_x u, x, t).$$

- Choose a grid of spatial points, x_n .
- Evaluate the function u on this grid: $u_n(t) = u(x_n, t)$.



- Approximate the spatial derivatives at the grid points

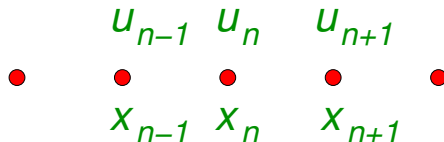
$$\partial_x u(x_n) = \sum_k D_{nk} u_k.$$

- Evaluate F at the grid points x_n in terms of the u_k : $F(u_k, x_n, t)$.

Numerical Solution of Evolution Equations

$$\partial_t u = F(u, \partial_x u, x, t).$$

- Choose a grid of spatial points, x_n .
- Evaluate the function u on this grid: $u_n(t) = u(x_n, t)$.



- Approximate the spatial derivatives at the grid points

$$\partial_x u(x_n) = \sum_k D_{nk} u_k.$$

- Evaluate F at the grid points x_n in terms of the u_k : $F(u_k, x_n, t)$.
- Solve the coupled system of ordinary differential equations,

$$\frac{du_n(t)}{dt} = F[u_k(t), x_n, t],$$

using standard numerical methods (e.g. Runge-Kutta).

Basic Numerical Methods

- Different numerical methods use different ways of choosing the grid points x_n , and different expressions for the spatial derivatives

$$\partial_x u(u_n) = \sum_k D_{nk} u_k.$$

Basic Numerical Methods

- Different numerical methods use different ways of choosing the grid points x_n , and different expressions for the spatial derivatives

$$\partial_x u(u_n) = \sum_k D_{nk} u_k.$$

- Most numerical groups use **finite difference** methods:
 - Uniformly spaced grids: $x_n - x_{n-1} = \Delta x = \text{constant}$.
 - Use Taylor expansions,

$$u_{n-1} = u(x_n - \Delta x) = u(x_n) - \partial_x u(x_n) \Delta x + \partial_x^2 u(x_n) \Delta x^2 / 2 + \mathcal{O}(\Delta x^3),$$

$$u_{n+1} = u(x_n + \Delta x) = u(x_n) + \partial_x u(x_n) \Delta x + \partial_x^2 u(x_n) \Delta x^2 / 2 + \mathcal{O}(\Delta x^3),$$

to obtain the needed expressions for $\partial_x u$:

$$\partial_x u(x_n) = \frac{u_{n+1} - u_{n-1}}{2\Delta x} + \mathcal{O}(\Delta x^2).$$

Basic Numerical Methods

- Different numerical methods use different ways of choosing the grid points \mathbf{x}_n , and different expressions for the spatial derivatives

$$\partial_x u(u_n) = \sum_k D_{nk} u_k.$$

- Most numerical groups use **finite difference** methods:
 - Uniformly spaced grids: $\mathbf{x}_n - \mathbf{x}_{n-1} = \Delta \mathbf{x} = \text{constant}$.
 - Use Taylor expansions,

$$u_{n-1} = u(\mathbf{x}_n - \Delta \mathbf{x}) = u(\mathbf{x}_n) - \partial_x u(\mathbf{x}_n) \Delta \mathbf{x} + \partial_x^2 u(\mathbf{x}_n) \Delta \mathbf{x}^2 / 2 + \mathcal{O}(\Delta \mathbf{x}^3),$$

$$u_{n+1} = u(\mathbf{x}_n + \Delta \mathbf{x}) = u(\mathbf{x}_n) + \partial_x u(\mathbf{x}_n) \Delta \mathbf{x} + \partial_x^2 u(\mathbf{x}_n) \Delta \mathbf{x}^2 / 2 + \mathcal{O}(\Delta \mathbf{x}^3),$$

to obtain the needed expressions for $\partial_x u$:

$$\partial_x u(\mathbf{x}_n) = \frac{u_{n+1} - u_{n-1}}{2\Delta \mathbf{x}} + \mathcal{O}(\Delta \mathbf{x}^2).$$

- Grid spacing decreases as the number of grid points N increases, $\Delta \mathbf{x} \sim 1/N$. Errors in finite difference methods scale as N^{-p} .

Basic Numerical Methods II

- A few groups (Caltech/Cornell, Meudon) use **spectral methods**.

Basic Numerical Methods II

- A few groups (Caltech/Cornell, Meudon) use **spectral methods**.
- Represent functions as finite sums: $u(\mathbf{x}, t) = \sum_{k=0}^{N-1} \tilde{u}_k(t) e^{ik\mathbf{x}}$.
- Choose grid points \mathbf{x}_n to allow efficient (and exact) inversion of the series: $\tilde{u}_k(t) = \sum_{n=0}^{N-1} w_n u(\mathbf{x}_n, t) e^{-ik\mathbf{x}_n}$.

Basic Numerical Methods II

- A few groups (Caltech/Cornell, Meudon) use **spectral methods**.
- Represent functions as finite sums: $u(\mathbf{x}, t) = \sum_{k=0}^{N-1} \tilde{u}_k(t) e^{ikx}$.
- Choose grid points \mathbf{x}_n to allow efficient (and exact) inversion of the series: $\tilde{u}_k(t) = \sum_{n=0}^{N-1} w_n u(\mathbf{x}_n, t) e^{-ikx_n}$.
- Obtain derivative formulas by differentiating the series:
$$\partial_x u(\mathbf{x}_n, t) = \sum_{k=0}^{N-1} \tilde{u}_k(t) \partial_x e^{ikx_n} = \sum_{m=0}^{N-1} D_{nm} u(\mathbf{x}_m, t).$$

Basic Numerical Methods II

- A few groups (Caltech/Cornell, Meudon) use **spectral methods**.
- Represent functions as finite sums: $u(\mathbf{x}, t) = \sum_{k=0}^{N-1} \tilde{u}_k(t) e^{ik\mathbf{x}}$.
- Choose grid points \mathbf{x}_n to allow efficient (and exact) inversion of the series: $\tilde{u}_k(t) = \sum_{n=0}^{N-1} w_n u(\mathbf{x}_n, t) e^{-ik\mathbf{x}_n}$.
- Obtain derivative formulas by differentiating the series:
 $\partial_x u(\mathbf{x}_n, t) = \sum_{k=0}^{N-1} \tilde{u}_k(t) \partial_x e^{ik\mathbf{x}_n} = \sum_{m=0}^{N-1} D_{nm} u(\mathbf{x}_m, t)$.
- Errors in spectral methods are dominated by the size of \tilde{u}_N .
- Estimate the errors (for Fourier series of *smooth* functions):

$$\begin{aligned} \tilde{u}_N &= \frac{1}{2\pi} \int_{-\pi}^{\pi} u(x) e^{-iNx} dx = \frac{1}{2\pi} \left(\frac{-i}{N} \right) \int_{-\pi}^{\pi} \frac{du(x)}{dx} e^{-iNx} dx \\ &= \frac{1}{2\pi} \left(\frac{-i}{N} \right)^p \int_{-\pi}^{\pi} \frac{d^p u(x)}{dx^p} e^{-iNx} dx \leq \frac{1}{N^p} \max \left| \frac{d^p u(x)}{dx^p} \right|. \end{aligned}$$

Basic Numerical Methods II

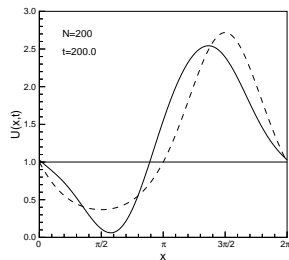
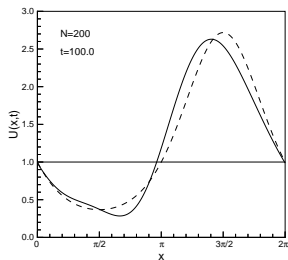
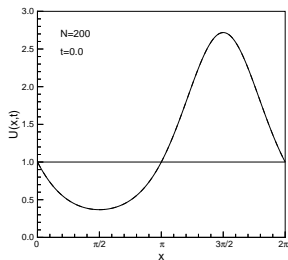
- A few groups (Caltech/Cornell, Meudon) use **spectral methods**.
- Represent functions as finite sums: $u(\mathbf{x}, t) = \sum_{k=0}^{N-1} \tilde{u}_k(t) e^{ik\mathbf{x}}$.
- Choose grid points \mathbf{x}_n to allow efficient (and exact) inversion of the series: $\tilde{u}_k(t) = \sum_{n=0}^{N-1} w_n u(\mathbf{x}_n, t) e^{-ik\mathbf{x}_n}$.
- Obtain derivative formulas by differentiating the series:
 $\partial_x u(\mathbf{x}_n, t) = \sum_{k=0}^{N-1} \tilde{u}_k(t) \partial_x e^{ik\mathbf{x}_n} = \sum_{m=0}^{N-1} D_{nm} u(\mathbf{x}_m, t)$.
- Errors in spectral methods are dominated by the size of \tilde{u}_N .
- Estimate the errors (for Fourier series of *smooth* functions):

$$\begin{aligned} \tilde{u}_N &= \frac{1}{2\pi} \int_{-\pi}^{\pi} u(x) e^{-iNx} dx = \frac{1}{2\pi} \left(\frac{-i}{N} \right) \int_{-\pi}^{\pi} \frac{du(x)}{dx} e^{-iNx} dx \\ &= \frac{1}{2\pi} \left(\frac{-i}{N} \right)^p \int_{-\pi}^{\pi} \frac{d^p u(x)}{dx^p} e^{-iNx} dx \leq \frac{1}{N^p} \max \left| \frac{d^p u(x)}{dx^p} \right|. \end{aligned}$$

- Errors in spectral methods decrease faster than any power of N .

Comparing Different Numerical Methods

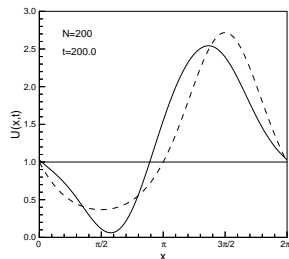
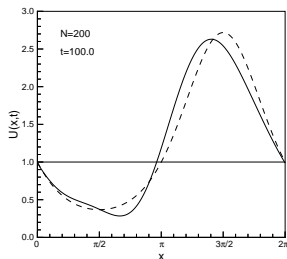
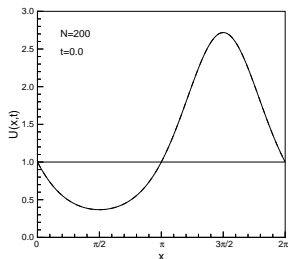
- Wave propagation with second-order finite difference method:



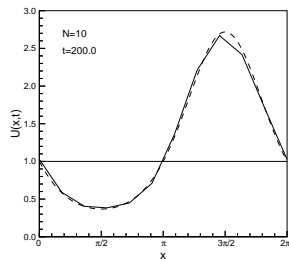
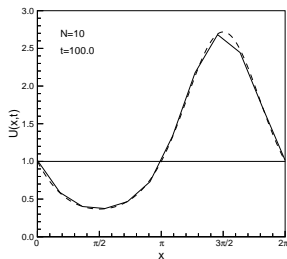
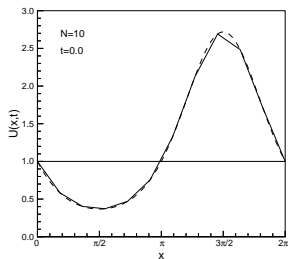
Figures from Hesthaven, Gottlieb, & Gottlieb (2007).

Comparing Different Numerical Methods

- Wave propagation with second-order finite difference method:



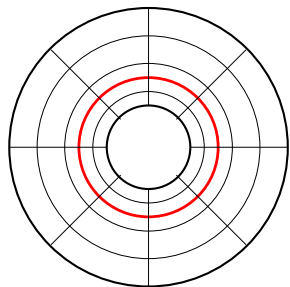
- Wave propagation with spectral method:



Figures from Hesthaven, Gottlieb, & Gottlieb (2007).

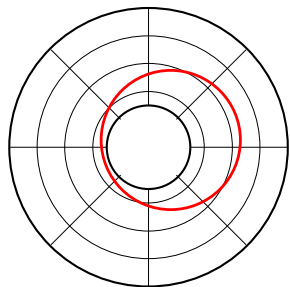
Moving Black Holes

- Black hole interior is not in causal contact with exterior. Interior is removed, introducing an excision boundary.



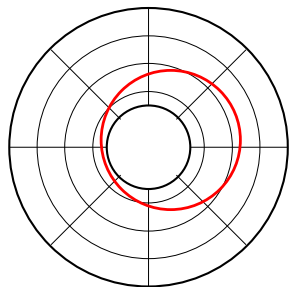
Moving Black Holes

- Black hole interior is not in causal contact with exterior. Interior is removed, introducing an excision boundary.



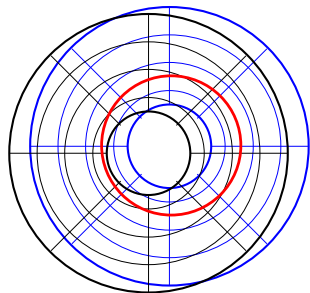
Moving Black Holes

- Black hole interior is not in causal contact with exterior. Interior is removed, introducing an excision boundary.
- Numerical grid must be moved when black holes move too far.



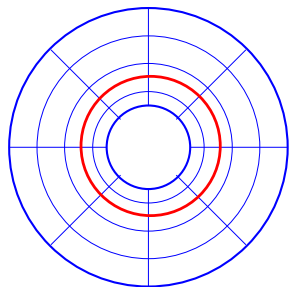
Moving Black Holes

- Black hole interior is not in causal contact with exterior. Interior is removed, introducing an excision boundary.
- Numerical grid must be moved when black holes move too far.



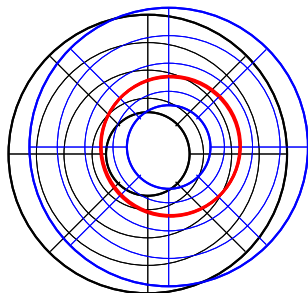
Moving Black Holes

- Black hole interior is not in causal contact with exterior. Interior is removed, introducing an excision boundary.
- Numerical grid must be moved when black holes move too far.



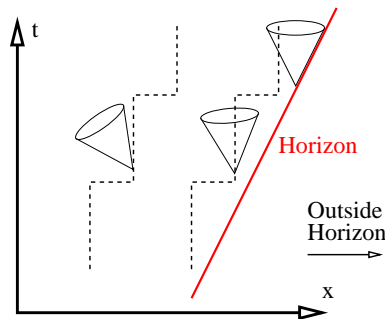
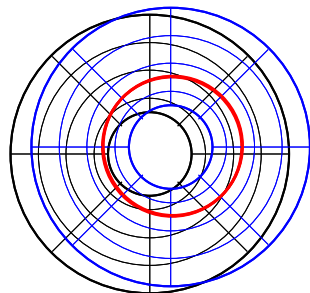
Moving Black Holes

- Black hole interior is not in causal contact with exterior. Interior is removed, introducing an excision boundary.
- Numerical grid must be moved when black holes move too far.
- **Problems:**
 - Difficult to get smooth extrapolation at trailing edge of horizon.



Moving Black Holes

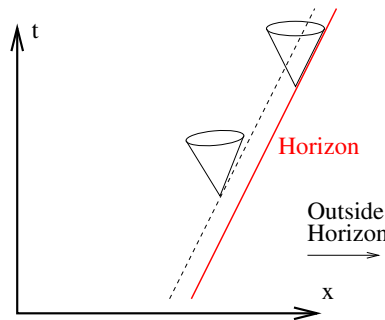
- Black hole interior is not in causal contact with exterior. Interior is removed, introducing an excision boundary.
- Numerical grid must be moved when black holes move too far.
- **Problems:**
 - Difficult to get smooth extrapolation at trailing edge of horizon.
 - Causality trouble at leading edge of horizon.



Moving Black Holes

- Black hole interior is not in causal contact with exterior. Interior is removed, introducing an excision boundary.
- Numerical grid must be moved when black holes move too far.
- **Problems:**
 - Difficult to get smooth extrapolation at trailing edge of horizon.
 - Causality trouble at leading edge of horizon.
- **Solution:**

Choose coordinates that smoothly track the motions of the centers of the black holes.



Horizon Tracking Coordinates

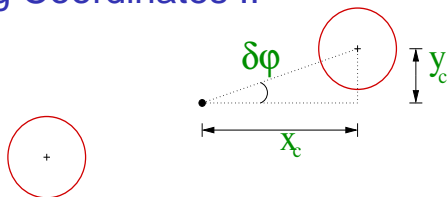
- Coordinates must be used that track the motions of the holes.
- A coordinate transformation from “inertial” coordinates, $(\bar{x}, \bar{y}, \bar{z})$, to “co-moving” coordinates (x, y, z) , consisting of a rotation followed by an expansion,

$$\begin{pmatrix} x \\ y \\ z \end{pmatrix} = e^{a(\bar{t})} \begin{pmatrix} \cos \varphi(\bar{t}) & -\sin \varphi(\bar{t}) & 0 \\ \sin \varphi(\bar{t}) & \cos \varphi(\bar{t}) & 0 \\ 0 & 0 & 1 \end{pmatrix} \begin{pmatrix} \bar{x} \\ \bar{y} \\ \bar{z} \end{pmatrix},$$

is general enough to keep the holes fixed in co-moving coordinates for suitably chosen functions $a(\bar{t})$ and $\varphi(\bar{t})$.

- Since the motions of the holes are not known *a priori*, the functions $a(\bar{t})$ and $\varphi(\bar{t})$ must be chosen dynamically and adaptively as the system evolves.

Horizon Tracking Coordinates II

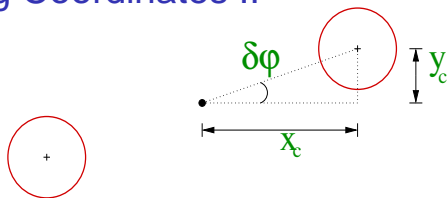


- Measure the co-moving centers of the holes: $x_c(t)$ and $y_c(t)$, or equivalently

$$Q^x(t) = \frac{x_c(t) - x_c(0)}{x_c(0)},$$

$$Q^y(t) = \frac{y_c(t)}{x_c(t)}.$$

Horizon Tracking Coordinates II



- Measure the co-moving centers of the holes: $x_c(t)$ and $y_c(t)$, or equivalently

$$Q^x(t) = \frac{x_c(t) - x_c(0)}{x_c(0)},$$

$$Q^y(t) = \frac{y_c(t)}{x_c(t)}.$$

- Choose the map parameters $a(t)$ and $\varphi(t)$ to keep $Q^x(t)$ and $Q^y(t)$ small.
- Changing the map parameters by the small amounts, δa and $\delta\varphi$, results in associated small changes in δQ^x and δQ^y :

$$\delta Q^x = -\delta a, \quad \delta Q^y = -\delta\varphi.$$

Horizon Tracking Coordinates III

- Measure the quantities $Q^y(t)$, $dQ^y(t)/dt$, $d^2Q^y(t)/dt^2$, and set

$$\frac{d^3\varphi}{dt^3} = \lambda^3 Q^y + 3\lambda^2 \frac{dQ^y}{dt} + 3\lambda \frac{d^2 Q^y}{dt^2} = -\frac{d^3 Q^y}{dt^3}.$$

The solutions to this “closed-loop” equation for Q^y have the form $Q^y(t) = (At^2 + Bt + C)e^{-\lambda t}$, so Q^y always decreases as $t \rightarrow \infty$.

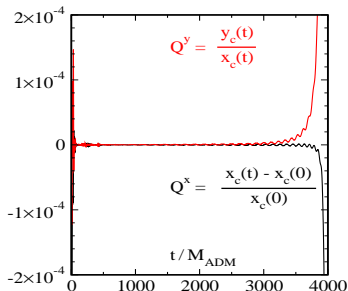
Horizon Tracking Coordinates III

- Measure the quantities $Q^Y(t)$, $dQ^Y(t)/dt$, $d^2Q^Y(t)/dt^2$, and set

$$\frac{d^3\varphi}{dt^3} = \lambda^3 Q^Y + 3\lambda^2 \frac{dQ^Y}{dt} + 3\lambda \frac{d^2Q^Y}{dt^2} = -\frac{d^3Q^Y}{dt^3}.$$

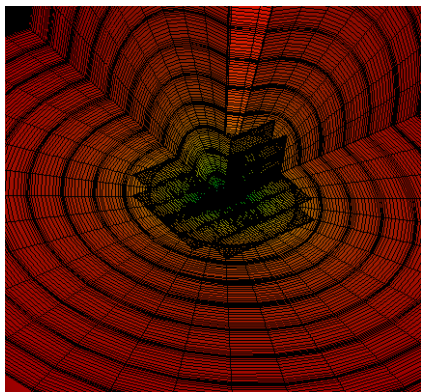
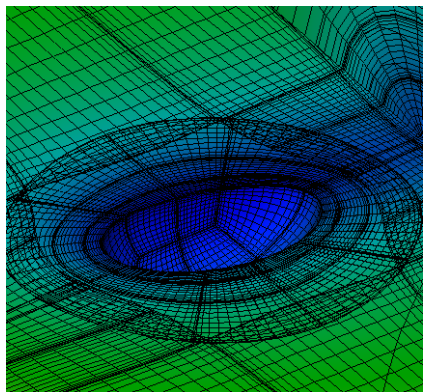
The solutions to this “closed-loop” equation for Q^Y have the form $Q^Y(t) = (At^2 + Bt + C)e^{-\lambda t}$, so Q^Y always decreases as $t \rightarrow \infty$.

- **This works!** We are now able to evolve binary black holes using horizon tracking coordinates until just before merger.



Caltech/Cornell Spectral Einstein Code (SpEC):

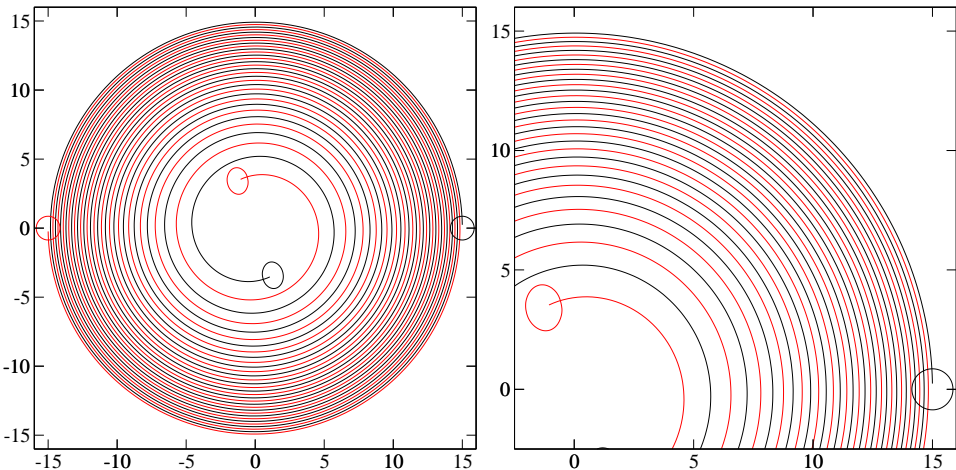
- Multi-domain spectral method.



- State of the art elliptic solver for computing BBH initial data, etc.
- Constraint damped “generalized harmonic” Einstein equations:
$$\square g_{ab} = F_{ab}(g, \partial g).$$
- Constraint-preserving, physical and gauge boundary conditions.

Evolving Binary Black Hole Spacetimes

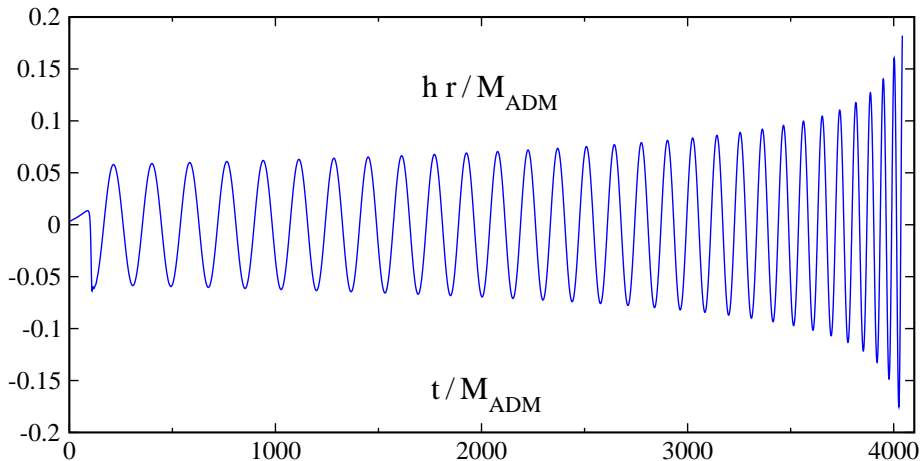
- We can now evolve binary black hole spacetimes with excellent accuracy and computational efficiency through many orbits.



Head-on Merger Movie

Gravitational Waveforms

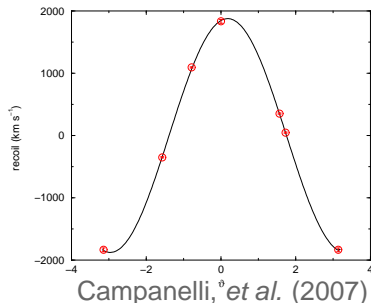
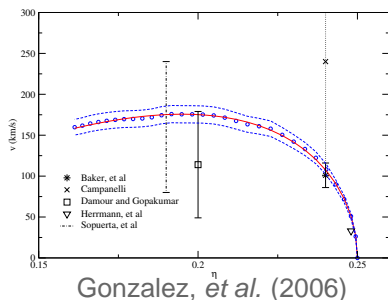
- High precision gravitational waveform for equal mass non-spinning BBH system.



Ψ_4 Movie

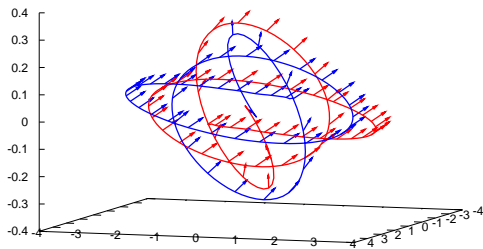
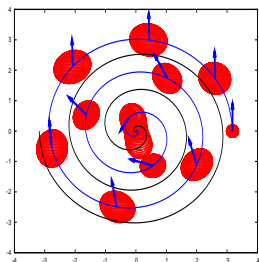
Black Hole Recoil

- Asymmetric binaries (unequal masses and/or non-aligned spins) emit linear momentum into GW; final merged hole recoils with non-zero velocity.
- Maximum recoil velocity for non-spinning holes is 175 km/sec.
- Recoil velocities of 2000 km/sec have been measured in spinning black hole simulations (estimated maximum ~ 4000 km/sec).
- Large recoils are probably rare (Schnittman & Buonanno 2007).



Spin Dynamics in Binary Black Hole Systems

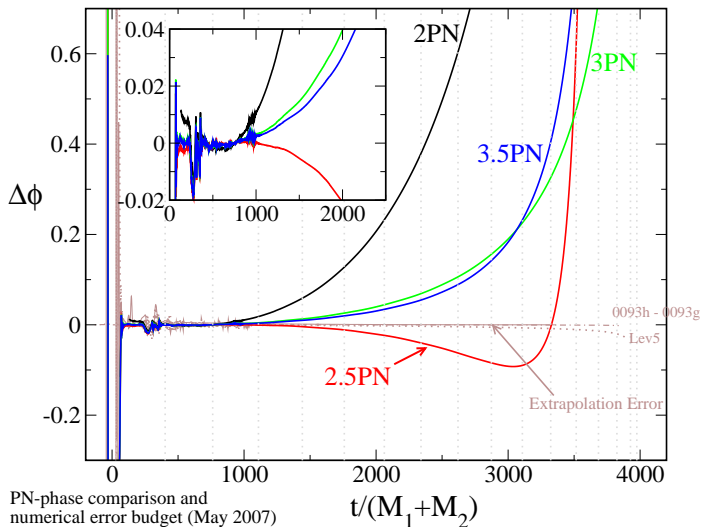
- Merger is delayed in BBHs with spins aligned with the orbital angular momentum; merger happens more quickly in binaries with anti-aligned spins.
- Complicated spin dynamics are observed in BBH mergers with non-aligned spins.



Campanelli, *et al.* (2007)

Post-Newtonian Waveform Calibration

- Preliminary comparisons of the numerical gravitational wave phase with predictions of various post-Newtonian orders.



Summary

- Advances in understanding the Einstein equations provide new formulations suitable for numerical evolutions: hyperbolic formulations with constraint damping and well posed initial-boundary value problems.
- High accuracy multi-orbit binary black hole simulations are now routine (but not yet cheap).
- Numerical waveforms suitable for LIGO data analysis are starting to be generated.
- Interesting non-linear dynamics of binary black hole mergers are beginning to be investigated.

